A FEM STUDY OF THE OVERLAPPING RATIO EFFECT ON SUPERPLASTIC FORMATION OF METAL MATRIX COMPOSITES

M. Tehrani *, A. Abedian **
*** M.Sc. Student, Aerospace Eng. Department, Sharif University of Technology;**
**** Associate Professor, Aerospace Eng. Department, Sharif University of Technology;**

Keywords: *3-D symmetric model, Finite Element Method (FEM), Metal Matrix Composites (MMCs), Overlapping Ratio (OR), Superplastic forming.*

Abstract

In aerospace applications structures weight is considered as a major performance parameter. One of the most effective manufacturing methods for weight reduction is superplastic forming. By this technique, not only the weight, but also the stress concentration, the cost, and the manufacturing time are noticeably reduced. Additionally, the components with complicated shapes could be formed in a single manufacturing step. Due to the wide demand for whiskers reinforced metal matrix composites (MMCs) in aerospace industries, many research works have been designed to extend the borders of superplastic forming to MMCs materials.

In the present study, a 3-D symmetric micromechanical finite element model is developed to predict the superplastic behavior of Al/SiC$_w$ composite. Here, the effects of fibers Overlapping Ratio (OR) on the superplastic forming process are highlighted. In most of the available numerical studies this phenomenon has been ignored. Here, the Internal Stress Superplasticity (ISS) mechanism is considered. This mechanism involves a thermal cycling load (e.g. 100°-450°-100°c, with 50s heating and 150s cooling period) accompanied by a constant biasing mechanical load (e.g. 2, 4, 7, 10 MPa). The effects of different overlapping ratios (i.e. 0.25 ≤ OR ≤ 1) on plastic strain response of the MMC are investigated.

According to the results, the total plastic strain, which is accumulated during 40 thermal cycles, increases in the range of overlapping ratio of 0.5 ≤ OR ≤ 1 and then decreases in the range of 0.25 ≤ OR ≤ 0.5. As it is seen, the effect of overlapping ratio on plastic strain response of the composite is more pronounced once the OR =0.5. In fact, it seems in ISS process, the location of whiskers relative to each other inside the matrix plays a key role.

1 Introduction

The low density and high modulus of whiskers reinforced Metal Matrix Composites (MMCs) have made these materials very attractive for the aerospace applications [1, 2]. But, it is so difficult to conform these materials into complex shapes because they exhibit very poor ductility and also they are often quite difficult to machine. In recent years, the borders of superplastic experience with conventional materials have been extended to the area of composite materials. Many experiments have been designed to explore and clarify the best mechanisms of superplastic forming in these materials [3-6]. The studies have indicated that the loading condition of simultaneous application of a thermal cycle and a low constant mechanical stress is the best way for enforcing MMCs to undertake superplastic forming.

Two of the well known mechanisms distinguished by these research studies are referred to as the Fine Structure Superplasticity (*FSS*) and the Internal Stress Superplasticity (*ISS*) [7-9]. The former applies to the materials with fine grain structures, while the latter applies to either the materials which go through a phase change under thermal cycling (like Ni-

Fe alloys), or the materials which possess different Coefficients of Thermal Expansions (*CTEs*) in different directions (like Zinc and α-Uranium) or include phases with different CTEs (like Al/SiC_w composites) [8]. It should be noted that for ISS regime, since the plasticity occurs by means of slip deformation mechanism, the size of grain is not of great importance.

Two different practical approaches which are distinguished based on their kind of loading, i.e. isothermal and thermal cycling, are employed for imposing superplastic forming by ISS mechanism [15]. For the first approach, which is more common in practice, the forming is performed in a constant temperature with relatively high strain rate. However, for the second method, which is so called thermal cycling superplasticity, the strain rate is low and in average it falls in the range of 10^{-5} to 10^{-4} s^{-1} [12].

Based on the results, the thermal cycling approach along with an external tensile mechanical stress, which is also considered to be small and constant, is employed here for superplastic forming of MMC materials [13]. Here, the difference in CTEs of the fiber and matrix creates large interfacial internal stresses, which depending on the characteristics of the applied thermal cycle, these stresses could increase to the values higher than the yield strength of the matrix causing plastic deformation in the composite. However, since a thermal cycling regime is used here, the plastic strain totally vanishes when the temperature is reserved in the next half of the cycle. However, application of a small tensile mechanical stress will bias the stress field that is generated during a full thermal cycle. This causes a small permanent plastic strain to accumulate with repeating the thermal cycle.

Regarding the interfacial internal stresses, a stress flow is observed throughout the matrix in which elongations of up to several hundred percentages could happen without any trace of irregularity or sharp changes in the cross section. In fact, the stress flow is highly dependent on the rate of plastic strain in the material. When this relationship happens to be linear, the conditions of Newtonian viscous flow will persist. This means the material behaves like glass, where it can experience a very large deformation without any sign of necking in the sample. This is best explained considering the *Backofen* Equation (1);

$$\begin{Bmatrix} \dot{\varepsilon} = k\sigma^n \\ or \\ \sigma = B\dot{\varepsilon}^m \end{Bmatrix} \quad (1)$$

where $m=1/n$ and is called strain rate sensitivity. For $n=1$ (or $m=1$) the relationship between $\dot{\varepsilon}$ and σ will be linear.

2 Geometry, Loadings, and Materials modeling

In order to reduce the cost of calculations and also overcoming the hardware and software limitations, it is necessary to adopt some simplification assumptions regarding the geometry modeling of the composite under consideration. The SEM photos of Al/SiC_w composite have shown that normally the added SiC whiskers to the Aluminum matrix are dispersed in the direction of the extrusion axis [3, 10]. The photos show that the misalignment of about 30% of the whiskers is limited to ±9.3° where the rest are more or less aligned. Therefore, it could be assumed that the fibers are of circular cross section and aligned as shown in Fig. 1.

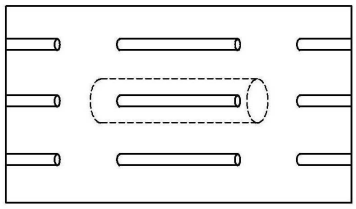

Fig. 1. Fibers placement inside the matrix [3, 10]

According to the previous research works, there are two common 3D micromechanical models which are widely used in superplasticity analyses. These two configurations are shown in Fig. 2. As it is seen in Fig. 2(a), there is one fiber at the center of each hexagonal pattern which is surrounded by six fibers at six corners. While, in the square pattern i.e. Fig. 2(b), there is a fiber at the center of a square which is

surrounded by four fibers. Here, it is assumed that the black-color fibers are fixed and the surrounded fibers can move regarding the different overlapping ratios considered. Here, the second configuration is more applicable because according to the cross sectional area of each fiber, the share of two fibers which carry load is equal [10].

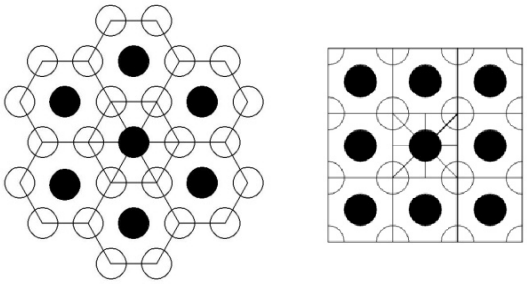

Fig. 2. Fibers configuration inside the matrix [10]

As shown in Fig. 3, the unit cell for the square pattern could be made by passing 5 planes through the composite introduced in Fig. 2(b). Despite the axisymmetric model which is used in [3], the presented model could simulate the longitudinal movement of fibers necessary to provide the required overlapping ratios. The black fiber is considered to be fixed and the white ones are moveable. Note that the OR value is controlled by the amount of adjacent fibers lengths that cover each other. For example for Fig. 4, *OR*=1.

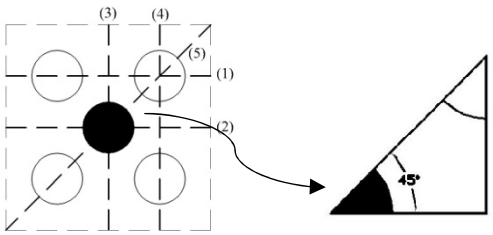

Fig. 3. The unit cell along with the applied BC's

Such an assumption makes it possible to simulate the whole composite with a 3-D symmetric micromechanical model considering appropriate boundary conditions which are presented in Fig. 4. To include the effects of the adjacent whiskers it is necessary to consider that the displacements of the nodes in the two planes of *ABDC* and *O'DC* are coupled in the *X*- and *Z*-directions, respectively. According to the applied planes of symmetry, the nodes in the *AOB*, *OO'DB*, and *OO'CA* planes have no displacement perpendicular to the planes. Finally, the *X* and *Y* displacement of the nodes on line *OO'* will be zero.

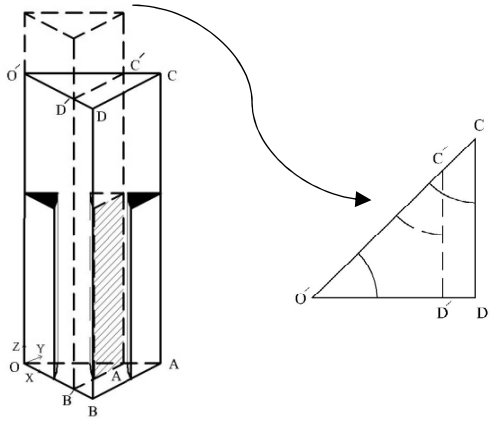

Fig. 4. Boundary conditions applied to the model

The fiber misalignment, interface debonding, and fiber and unit cell geometric aspect ratios, which could also affect the plastic strain, are ignored here.

As for the meshing, uniform nonlinear elements are considered. The *Solid95* of *ANSYS* element library, which is a nonlinear elasto-viscoplastic element, is used for the geometry meshing. The fiber volume fraction (V_f) is calculated as shown by Eq. (2)

$$V_f = \frac{V_{fiber}}{V_{unit\ cell}} = \frac{2(\frac{1}{8})\pi r^2 l_f}{\frac{1}{2} b^2 l_{unit\ cell}} \quad (2)$$

where r and b are the fiber and the unit cell radii, and l_f and $l_{unit\ cell}$ are the fiber and the unit cell length, respectively. Here, the volume fraction of 20 percent, r_f = 10, and l_f = 40 are considered.

As for the loading, according to the literature available on the experimental superplasticity [8], it is assumed that a thermal cycling regime as in Fig. 5 is applied to the model.

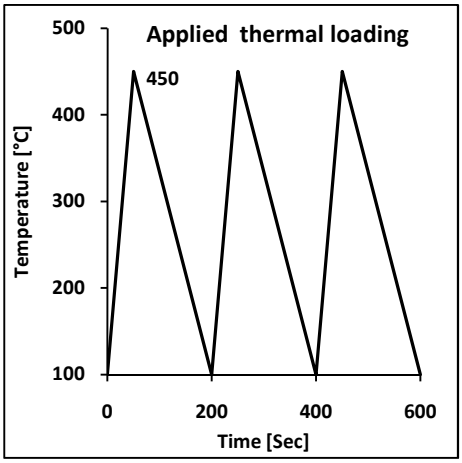

Fig. 5. Profile of the applied thermal cycles [8]

For the heating phase of the cycle, the composite is heated between 100°*C*- 450°*C* in 50 seconds, while it is cooled down to 100°*C* from the maximum of 450°*C* during 150 seconds [8]. This thermal cycle is accompanied with a constant longitudinal small mechanical stress of magnitude 2, 4, 7, and 10 *MPa* [18] to enforce the plastic strain accumulation in each thermal cycle.

As explained before, in most of the previous research works the material properties were considered to be constant with the temperature change [3, 10]. However, regarding the maximum temperature of 450°*C*, it is not reasonable to go forward with such an assumption any more. Constant properties assumption may lead to rough results which do not correlate with experimental results. Therefore, to achieve more accurate results, here the following changes in properties with temperature as presented in Tables 1 and 2, for the fiber and matrix are considered, respectively.

Table 1: Material properties of the SiC_w [4, 5]

Temp. (°*C*)	**0**	**50**	**100**	**200**	**300**	**400**	**500**
E (*Gpa*)	450	450	450	450	450	450	450
ν	0.18	0.18	0.18	0.18	0.18	0.18	0.18
σ_y (*MPa*)	***	***	***	***	***	***	***
α (*ppm/k*)	2.7	2.8	3.1	4.15	4.7	5.1	5.3

Table 2: Material properties of the Al2024 [4, 5]

Temp. (°*C*)	**0**	**50**	**100**	**200**	**300**	**400**	**500**
E (*Gpa*)	72	69	67	64	59	54	49
ν	0.32	0.33	0.34	0.35	0.37	0.38	0.39
σ_y (*MPa*)	33.5	33	32	24	14.5	10.5	9
α (*ppm/k*)	22.9	23.6	24.2	25.7	27.7	30.4	31.7

As it is shown in Table 1, the yield stress property of fiber is not considered because in this study it is assumed that fibers remain elastic during the whole process, while the Al2024 matrix behaves in an elastic-perfectly plastic manner [16].

3 Results and discussion

As mentioned before, for the ISS mechanism, with increasing the number of applied thermal cycle in presence of the mechanical load, the plastic strain starts to accumulate. Based on the results published in [9], with the linear relationship of the accumulated plastic strain (ε_p) with the number of cycles (N) for all the constant mechanical load cases, the strain rate ($\dot{\varepsilon}$) can be calculated from Eq. (3);

$$\dot{\varepsilon} = \frac{d\varepsilon_p}{dN}.\frac{1}{\tau} \tag{3}$$

where $d\varepsilon_p$ represents the accumulated plastic strain in a given number of cycles (i.e. dN) and τ indicates the period of the applied thermal cycle. Then the log-log scale plot of $\dot{\varepsilon}$ values vs. the applied mechanical load indicates a power law type relationship (as in Eq. (1)) for the material behavior.

The calculated magnitude of the power of Eq. (1) depends on the position of selected element of the model which strain data is collected from. Replacing the element with, for example, another element placed at the tip corner of the fiber, some great differences in the values of the strain could be realized. Therefore, the need for a general data collection is clear and also necessary to develop. This task is fulfilled here with the use of averaging method by Hsueh in [19] which was first used for calculation of the average elastic strain. But, here, it is done with applying some modifications to the proposed procedure [10]. The average of elemental ε_p was incorporated in to the Eq. (4);

$$\bar{\varepsilon}^p = \frac{\sum_{i=1}^{n} \bar{\varepsilon}^p{}_i \, \mathrm{v}_i}{\sum_{i=1}^{n} \mathrm{v}_i} \tag{4}$$

where $\bar{\varepsilon}^p$ represents the average plastic strain over the entire model, n represents the element numbers, v_i is the volume of the ith element, and $\bar{\varepsilon}^p{}_i$ is the average elemental plastic strain.

Fig. 5 presents the average plastic strain vs. the number of cycles (time) for constant stress of σ =10MPa considering the effects of fibers overlapping. As the figure shows, seven different overlapping ratios in the region of $0.25 \leq OR \leq 1$ are investigated. The results show that by decreasing the OR from 1 to 0.5 the plastic strain increases and then by decreasing again from 0.5 to 0.25 the plastic strain decreases to the former values. In other words, by moving one of the corner fibers against the fixed one, the plastic strain starts to increase from 0.104 to 0.142 and then decreases to the values for OR= 0.625 when OR reaches 0.25.

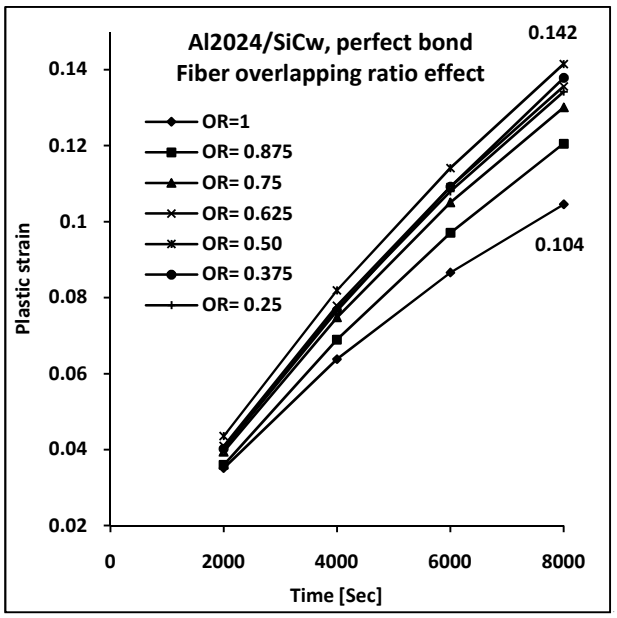

Fig. 5. Plastic strain vs. time response for different overlapping ratios under the 10 MPa tensile loading

It should be noted that regarding the specified V_f and fiber and unit cell aspect ratios, it is not possible to simulate the effect of overlapping ratio in the range of 0.25 to 0. Fig. 6 presents the plastic strain vs. overlapping ratio at 40th loading cycle (time= 8000 sec.) for mechanical loading of 10 MPa. As it is seen, the dashed line which interpolates the plastic strain results, has its maximum magnitude at OR= 0.5.

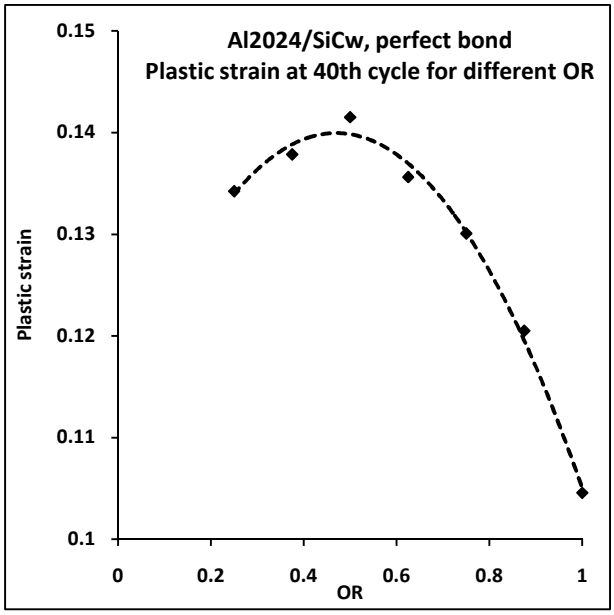

Fig. 6. The plastic strain response vs. overlapping ratios at 40th cycle

Fig. 7 presents the geometry of overlapping of two fibers inside the matrix. The two parameters of d_1 and d_2 are the distance of moving fiber's ends relative to the fixed fiber's end. As it is shown, once the moving fiber is placed in different overlapping ratios, the values of d_1 and d_2 are changed. The OR= 1 indicates the minimum of d_1 and the maximum of d_2. Accroding to the plastic strain flow patterns through the matrix, it seems that the fiber's ends interupt the flow and decrease the plastic strain. When d_1= d_2, as shown in Fig. 7, this interference is minimum and lead into the maximum plastic strain. In the other word, for OR= 0.5 the plastic strain flow is optimum.

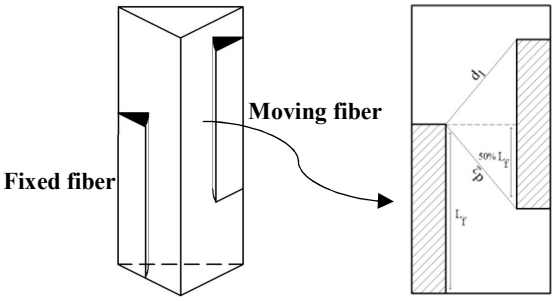

Fig. 7. Schematic fibers overlapping geometry

By converting Eq. (1) to the logaritmic form, Eq. (5) can be obtained;

$$\dot{\varepsilon} = k\sigma^n \rightarrow \log \dot{\varepsilon} = \log k + n \log \sigma \qquad (5)$$

where $log\dot{\varepsilon}$ is logaritmic averaged plastic strain rate, $logk$ is a constant term, and $log\sigma$ is logaritmic applied stress. To obtain the power of stress (n) in *Backoften* equation a log-log graph can be employed in which the slope of the first order line is interpreted as the power. Fig. 8 shows the plastic strain response of the model with *OR*= 0.5 under four different mechanical tensile stresses of 10, 7, 4, and 2 *MPa* during 40 thermal cycles. Based on the FEM results, for all 4 cases of constant stress considered, the rate of plastic strain accumulation is slightly decreased over the time. However, according to Fig. 5, it should be noted that this decrease in plastic strain rate for *OR*= 0.5 is lower in comparison with the case where *OR*= 1 was considered.

According to Eq. (5), which introduces a unique $\dot{\varepsilon}$, the average of $\dot{\varepsilon}$ should be considered. The dashed lines introduced in Fig. 8 presents the first order interpolation of plastic strain passed through the collected FEM data. The slopes of these lines, which are the coefficients of X in the presented line equations, indicate the average plastic strain rate.

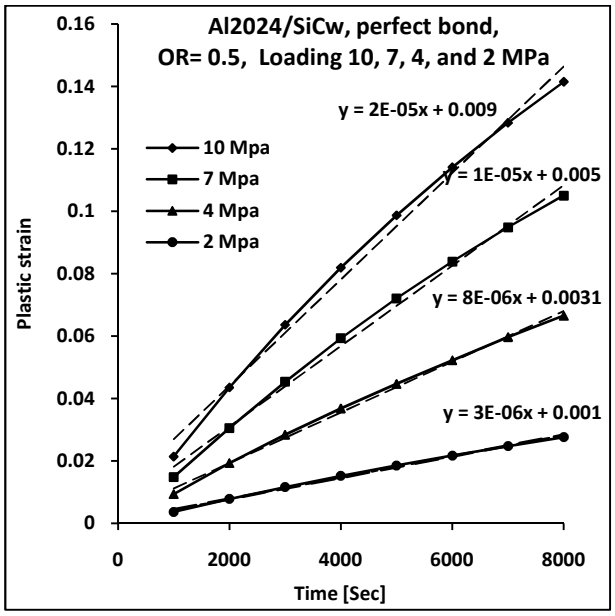

Fig. 8. Plastic strain vs. number of cycles for different constant mechanical loads considering *OR*= 0.5

As shown in the Fig. 9, the slope of the log-log graph of the plastic strain rate vs. applied mechanical stress is equal to n. As mentioned before, once n approaches to 1, the matrix experiences Newtonian viscous flow in which the material could be formed into the complex shapes with the minimum of necking.

In this figure the experiment results [8], the results of FEM model with *OR*= 0.5, and *OR* =1 as a *Reference Process* are compared. The obtained stress powers (n) for these three cases are 1.52, 0.99, and 0.81, respectively. As it is seen, the experimental results correlate better with the FEM results of the model with *OR*= 0.5. Therefore, including the overlapping ratio effect can effectively change the results.

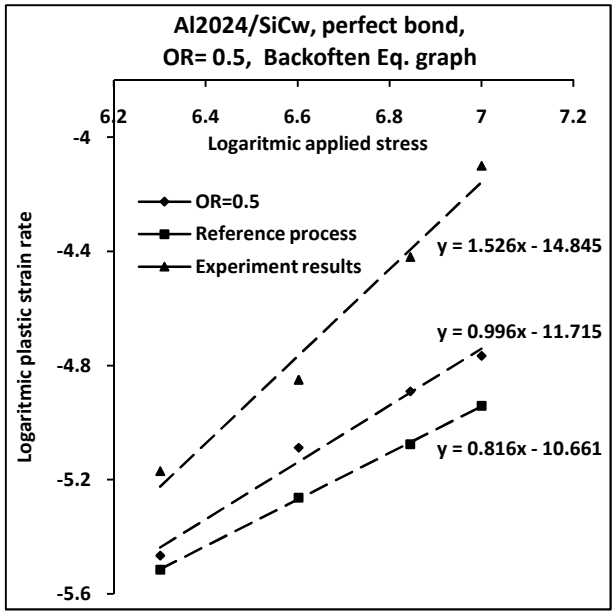

Fig. 9. Applied stress vs. plastic strain rate in log-log scale for *OR*= 1 (reference process) and *OR*= 0.5 compared with the experimental results [8]

Furthermore, according to the results, the value of n in experimental data is equal to 1.52 which is much more than the ideal magnitude of 1 obtained form finite element simulation. This difference indicates that the perfect plastic behavior of Aluminum matrix considered in the simulation is not valid in the experiment. Therefore, the Newtonian viscous flow could happen only in the FEM model which lead in to the powers close to 1.

3 Conclusions

Considering the results obtained from the FEM modeling of superplastic forming of MMCs, the followings could be concluded:

1- The 3D symmetric FEM model could predict the superplastic behavior of the MMCs to a great extent.

2- To obtain more accurate results and closer to experimental data it is necessary to consider the effect of fiber overlapping ratio.

3- It is now clear that the most important interference in the superplastic flow through the matrix is caused by fiber's end which highly affects the magnitude of plastic strain and also plastic strain rate.

4- The FEM results of the model with *OR*= 0.5 correlates better with experimental results and presents the optimum plastic strain flow inside the matrix.

References

[1] Xing H., Wang, C., Zhang, K., and Wang, Z., 2004. "Recent development in the mechanics of superplasticity and its applications", *Journal of Material Processing Technology*, pp. 196-202.

[2] Barens, A. J., 2001, "Industrial applications of superplastic forming; trends and prospects", *Materials Science forum*, Vols. 357-359.

[3] Abedian, A., Barakati, A., and Malekpour, A., 2006, "Effect of geometry aspects on the simulation of superplasticity in metal matrix composites", 25th ICAS conference.

[4] Huang, Y. D., Hort, N., Dieringa, H., Kainer, K. U., 2005, "Analysis of instantaneous thermal expansion coefficient curve during thermal cycling in short fiber reinforced AlSi12CuMgNi composites", *Journal of Composite Science and Technology*, 65 137-147.

[5] Nam, T., Requena, G., Degischer, P., 2008, "Thermal expansion behavior of aluminum matrix composites with densely packed SiC particles", *Journal of Composites*, Part A 39 856–865.

[6] Balasivanandha Prabu, S., Karunamoorthy, L., Kandasami, G.S., 2004, "A finite element analysis study of micromechanical interfacial characteristics of metal matrix composites", *Journal of Material Processing Technology*, 992-997.

[7] Guozheng, K., Sujuan, G., Cheng, D., 2006, "Numerical simulation for uniaxial cyclic deformation of discontinuously reinforced metal matrix composites", *Journal of Material Science and Engineering A*, Vol. 426, 66-76.

[8] Hong, S., Sherby, O., Divecha, A., Karmarker, S., and McDonald, B., 1988, "Internal stress superplasticity in Al2024-SiC whisker reinforced composites", *Journal of Composite Materials*, Vol. 22, pp. 102-123.

[9] Han, N. L., Wang, Z. G., Yang, J. M., Zhang, G. D., 2002, "Plastic-strain cyclic response of SiC particulate reinforced aluminum composites", *Journal of Material Science and Engineering*, A337, 140-145.

[10] Mondali, M., Abedian, A., pahlavanpour, M., 2006, "Finite element analysis of the fiber offsetting effects on the creep behavior of MMCs", CST Conference.

[11] Yang, Q., Qin, Q., 2001, "Fiber interactions and effective elasto-plastic properties for short-fiber composites", *Journal of Composite structures*, Vol. 54, 523-528.

[12] Nieh, T. G., Wadsworth, J., and Sherby O. D., 1997, "Superplasticity in metals and ceramics", *Cambridge University Press*.

[13] Kitazono, K., Hirasaka, R., Sato, E., Kuribayashi, K., and Motegi, T., 2001, "Internal stress superplasticity in anisotropic polycrystalline materials", *Acta Materialia*, pp. 473-486.

[14] Yeargadda, P. K., Gudimetla, P., and Adam, C., 2004, "Finite element analysis of high Strain rate superplastic materials", *Journal of Materials Processing Technology*.

[15] Chan, K. C., Tong, G. Q., 2001, "Strain rate sensitivity of a high-strain-rate superplastic Al606/SiC_w composite under uniaxial equibiaxial tension", *Materials Letters*.

[16] Horest, J. J., Salienko, N. V., and Spoormaker, J. L., 1998, "Fiber-Matrix debonding stress analysis for short fiber-reinforced materials with matrix plasticity", *FEM and Experimental verification*, *Composites part A*.

Contact Author Email Address

abedian@sharif.edu

Copyright Statement